Interplay of non-Hermitian skin effects and Anderson localization in nonreciprocal quasiperiodic lattices

Hui Jiang,[1,2] Li-Jun Lang,[3,*] Chao Yang,[1,2] Shi-Liang Zhu,[4,3] and Shu Chen[1,2,5,†]

[1]*Beijing National Laboratory for Condensed Matter Physics, Institute of Physics, Chinese Academy of Sciences, Beijing 100190, China*

[2]*School of Physical Sciences, University of Chinese Academy of Sciences, Beijing 100049, China*

[3]*Guangdong Provincial Key Laboratory of Quantum Engineering and Quantum Materials, SPTE, South China Normal University, Guangzhou 510006, China*

[4]*National Laboratory of Solid State Microstructures and School of Physics, Nanjing University, Nanjing 210093, China*

[5]*The Yangtze River Delta Physics Research Center, Liyang, Jiangsu 213300, China*

(Received 27 January 2019; revised manuscript received 15 July 2019; published 2 August 2019)

Non-Hermiticity from nonreciprocal hoppings has been shown recently to demonstrate the non-Hermitian skin effect (NHSE) under open boundary conditions (OBCs). Here we study the interplay of this effect and the Anderson localization (AL) in a *nonreciprocal* quasiperiodic lattice, dubbed nonreciprocal Aubry-André model, and a *rescaled* transition point is exactly proved. The nonreciprocity can induce not only NHSEs but also the asymmetry in localized states, characterized by two Lyapunov exponents. Meanwhile, this transition is also topological, in the sense of a winding number associated with complex eigenenergies under periodic boundary conditions (PBCs), establishing a *bulk-bulk* correspondence. This interplay can be realized straightforwardly by an electrical circuit with *only* linear passive RLC components instead of elusive nonreciprocal ones, showing the transport of a continuous wave undergoes a transition between insulating and amplifying. This paradigmatic scheme can be immediately accessed in experiments even for more nonreciprocal models and will definitely inspire the study of interplay of NHSEs and ALs as well as more other quantum/topological phenomena in various systems.

DOI: 10.1103/PhysRevB.100.054301

I. INTRODUCTION

Anderson localization (AL) [1] is an old but everlasting topic in condensed matter physics, which reveals a mechanism of insulation due to the destructive interference of multiple scattered waves induced by randomness [2,3]. This fundamental phenomenon has been experimentally observed for electronic spins [4,5], light [6–9], microwave [10–12], sound [13], and cold atoms [14–16]. In one dimension, AL occurs for any infinitesimal disorder [1–3], but at a finite point in quasiperiodic systems, such as the Aubry-André (AA) model [17]. This quasiperiodicity also has a profound connection to topology [18–22]: The AA model can be mapped to the well-known Hofstadter model [23] with an external periodic parameter as a synthetic dimension and thus relates to the Thouless pumping [24–27].

On the other hand, non-Hermiticity [28] has been studied intensively for years with the aid of the fast development of topological photonics [29–31]; it exhibits rich phenomena without Hermitian counterparts, e.g., $\mathcal{PT}$ symmetry breaking [32–34], exceptional points [35–39], etc. Especially, the non-Hermitian topology is attracting special attention for the violation of conventional bulk-boundary correspondence of Hermitian systems, and new ways of defining topology are needed [40–63]. Besides the on-site gain/loss, nonreciprocal hoppings can also bring in non-Hermiticity [49–59] with exotic features, such as non-Hermitian skin effects (NHSEs) under open boundary conditions (OBCs), which is helpful to understand the breakdown of bulk-boundary correspondence.

Among references, effects of non-Hermiticity on ALs have been studied in different contexts [64–74], but the discussion on the interplay of NHSEs and ALs with accompanying topological transitions is still lacking. Thus, natural questions arise: What is the fate of topological NHSEs in the presence of quasiperiodic potentials? Any transition inherited from the AL in Hermitian AA models? Answering these questions and further experimentally observing related exotic phenomena would be of importance and attractive to both communities of non-Hermitian quantum mechanics and condensed matter physics.

In this paper, we address the above questions in the AA model with nonreciprocal hoppings, dubbed *nonreciprocal AA model*, and indeed find a transition of NHSEs and ALs under OBCs with an analytically proved *rescaled* transition point inherited from the Hermitian counterpart. Affected by the nonreciprocity, besides NHSEs under OBCs, the Anderson localized states become asymmetric with respect to the localization center, characterized by *two* Lyapunov exponents. Meanwhile, this transition is topological, in the sense of a winding number associated with complex eigenenergies under periodic boundary conditions (PBCs) [54], which can

*ljlang@scnu.edu.cn
†schen@iphy.ac.cn

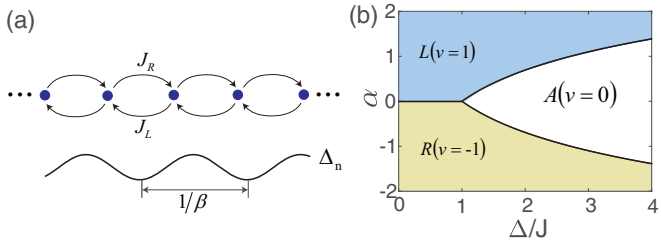

FIG. 1. (a) Sketch of the nonreciprocal AA model. (b) Phase diagram. The phase boundaries are determined by $\Delta/J = e^{|\alpha|}$ and $\alpha = 0$. Under OBCs, $\{L, R, A\}$ represent the left-skin, right-skin, and Anderson localized phases, respectively. The winding number ν is defined in the text. Under PBCs, only regions L and R have imaginary eigenenergies.

well distinguish the different skin phases and the localized phase under OBCs, establishing a *bulk-bulk* correspondence. In the end, to demonstrate the interplay, an electrical circuit is designed with *only* linear passive RLC components, which undoubtedly shows the transition through the transport of continuous waves between insulating and amplifying. Due to the lacking of experimental realizations of NHSEs in electrical circuits [75–83] as well as other platforms, this paradigmatic scheme provides a practical way to access it and can be directly used for more nonreciprocal models. Our work can also be generalized to other tunable artificial systems, such as photonics [29,30], ultracold atoms [84], and superconducting circuits [85], and thus will definitely inspire the study of interplays of NHSEs and other quantum/topological phenomena in these various systems.

II. NON-RECIPROCAL AA MODEL

The Hamiltonian of the nonreciprocal AA model [Fig. 1(a)] reads

$$\hat{H} = \sum_n (J_R|n+1\rangle\langle n| + J_L|n\rangle\langle n+1| + \Delta_n|n\rangle\langle n|), \quad (1)$$

where $J_{R(L)}$ is the right(left)-hopping amplitude, and $\Delta_n = 2\Delta\cos(2\pi\beta n)$ is an on-site quasiperiodic potential with Δ, without loss of generality, set positive and β usually taken to be an irrational number, say, the inverse of the golden ratio $(\sqrt{5}-1)/2$ for infinite systems. For finite systems with site number $N = F_{n+1}$, where F_n is the nth Fibonacci number, because $\lim_{n\to\infty} F_n/F_{n+1} = (\sqrt{5}-1)/2$, we usually take the rational number $\beta = F_n/F_{n+1}$, preserving the quasiperiodicity. For simplicity, we restrict the hoppings to be positive, which can be parameterized as $J_R = Je^{-\alpha}$, $J_L = Je^{\alpha}$ with $J > 0$ and α both real, unless mentioned otherwise. The nonreciprocity of hoppings ($\alpha \neq 0$) leads to the non-Hermiticity of the model, different from the non-Hermitian models based on the on-site gain/loss.

It is well known that, in the Hermitian case ($\alpha = 0$), AL occurs at $\Delta/J = 1$ for infinite systems due to the self-duality [17]: The extended states for $\Delta/J < 1$ become exponentially localized when $\Delta/J > 1$ with the form $|\psi\rangle \propto \sum_n e^{-\eta|n-n_0|}|n\rangle$, where n_0 is the index of the localization center, and $\eta = \ln(\Delta/J) > 0$ is the Lyapunov exponent, i.e., the inverse of the decaying length.

Deviated from the Hermitian limit, the transition should be extended to the nonreciprocal case ($\alpha \neq 0$). To catch a glimpse of the nonreciprocity effect on the transition, we can quickly look into the two limits of the Hermitian case: (1) For the state fully localized at one site, i.e., $\Delta/J \to \infty$, because the sites are decoupled, the nonreciprocal hoppings have no effect on the state. (2) For the state extended through all sites, i.e., $\Delta/J \to 0$, under OBCs the nonreciprocal hoppings will accumulate the state to one boundary, i.e., the NHSE, depending on $\mathrm{sgn}(\alpha)$ [50]. Apparently, at least under OBCs, the nonreciprocal AA model should undergo a transition between the skin phase and the localized phase.

III. INTERPLAY OF NON-HERMITIAN SKIN EFFECT AND ANDERSON LOCALIZATION UNDER OBCS

To understand ALs in the nonreciprocal AA model, Hamiltonian (1) under OBCs can be rewritten in a biorthogonal basis as $\hat{H} = \sum_{mn} h_{mn}|m\rangle\langle n| = \sum_{mn} h'_{mn}|\tilde{m}_R\rangle\langle\tilde{n}_L|$, where $|\tilde{m}_R\rangle \equiv e^{-\alpha m}|m\rangle$ and $\langle\tilde{n}_L| \equiv \langle n|e^{\alpha n}$ are the scaled basis in the right and left spaces, respectively, satisfying the biorthogonal condition $\langle\tilde{n}_L|\tilde{m}_R\rangle = \delta_{mn}$. Via this transformation, the non-Hermitian matrix h becomes a Hermitian one,

$$h' = \begin{pmatrix} \Delta_1 & J & & \\ J & \Delta_2 & J & \\ & \ddots & \ddots & \ddots \\ & & J & \Delta_N \end{pmatrix}, \quad (2)$$

which is just the matrix representation of the Hermitian AA model with $J = \sqrt{J_L J_R}$ being the amplitude of the *reciprocal* hoppings. This transformation also reveals the fact that all eigenenergies of Hamiltonian (1) are real, because h and h' are similar with the relation $h' = ShS^{-1}$, where $S = \mathrm{diag}(e^{\alpha}, e^{2\alpha}, ..., e^{N\alpha})$ is a similarity matrix with exponentially decaying diagonal entries.

As mentioned before, the Hermitian AA model represented by h' undergoes AL at $\Delta/J = 1$. Take ψ' to be the eigenvector of h'. Mathematically, the right eigenvector of h satisfies $\psi = S^{-1}\psi'$, which clearly shows how the nonreciprocity affects the state in the two phases of h': For extended states, S^{-1} exponentially accumulates the wave functions to one boundary, i.e., the NHSE; for localized states, the wave functions,

$$\psi_n \propto \begin{cases} e^{-(\eta+\alpha)(n-n_0)}, & n > n_0 \\ e^{-(\eta-\alpha)(n_0-n)}, & n < n_0 \end{cases}, \quad (3)$$

manifest different decaying behaviors on both sides of the localization center with two Lyapunov exponents $\eta \pm \alpha$. These results are consistent with our previous limit analysis, reflecting the *interplay* of NHSEs and ALs. According to Eq. (3), when $\eta \leqslant |\alpha|$ delocalization occurs on one side and then skin modes emerge to the boundary on the same side, from which the boundary of skin/localized phases is given by

$$\Delta/J = e^{|\alpha|} \text{ or } \Delta/\max(J_L, J_R) = 1. \quad (4)$$

This transition is similar to the Hermitian case but determined by the larger hopping, which also determines to which skin the wave functions will accumulate after delocalization, and thus, the Hermitian case ($\alpha = 0$) separates the left-skin ($\alpha > 0$) and right-skin ($\alpha < 0$) phases. Figure 1(b) shows the whole

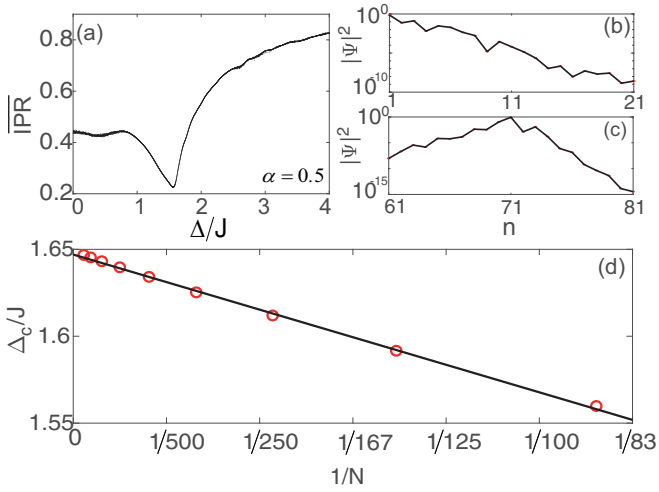

FIG. 2. (a) $\overline{\mathrm{IPR}}$ vs Δ/J for $\alpha = 0.5$ under OBCs. The deep dive at $\sim$1.56 divides the skin and localized phases. The calculation is carried on with $N = 89$ and $\beta = 55/89$. (b),(c) The profiles of eigenstates of 10th lowest $|E|$ in (a), showing the left-skin state and the asymmetric localized state at $\Delta/J = 0.5$ and 3, respectively. (d) Finite-size scaling analysis for the minimum $\overline{\mathrm{IPR}}$, Δ_c/J (circles), of different lengths with the linear fitting (line), showing the asymptotic value 1.647 ± 0.001 when $N \to \infty$.

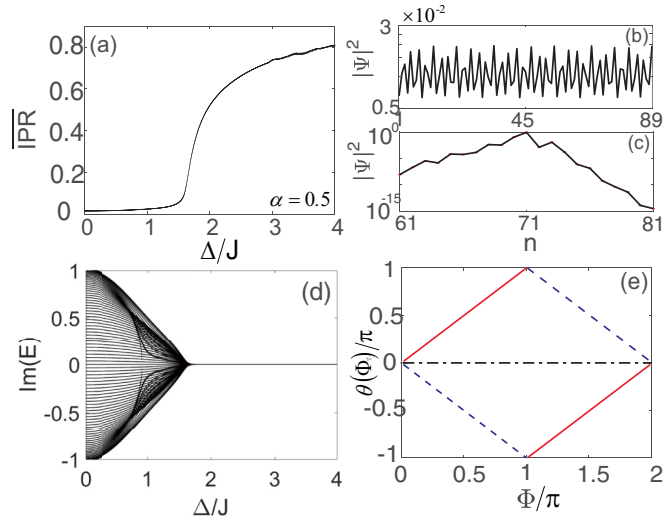

FIG. 3. (a)–(c) The same setting as in Figs. 2(a)–2(c) but under PBCs, showing the transition between extended and localized phases. (d) The imaginary parts of all eigenenergies in (a), indicating only extended states have complex energies. (e) $\theta(\Phi)$ for $(\alpha, \Delta/J) = (0.5, 0.5)$ (solid red), $(-0.5, 0.5)$ (dashed blue), and (0,3) (dash-dotted black), which, respectively, correspond to $\nu = +1$, -1, and 0 in Fig. 1(b).

phase diagram. As a demonstration, we calculate the averaged inverse participation ratios (IPRs) over all right eigenstates of $\hat{H}$ under OBCs,

$$\overline{\mathrm{IPR}} = \frac{1}{N}\sum_{s=1}^{N} \mathrm{IPR}_s = \frac{1}{N}\sum_{s=1}^{N} \frac{\sum_n |\langle n|\psi_s\rangle|^4}{(\langle\psi_s|\psi_s\rangle)^2}, \tag{5}$$

where $|\psi_s\rangle$ is the sth right eigenstate of $\hat{H}$. A state with $\mathrm{IPR} = 1$ is completely localized at a single site, while it is homogeneously distributed through all sites with $\mathrm{IPR} = 1/N$. Different from the extended phase with small IPRs of the Hermitian case, the skin phase should have larger values due to its boundary-localization nature. Therefore, the transition point should correspond to the most extended case, i.e., the smallest $\overline{\mathrm{IPR}}$. As expected, a deep dive at $\sim$1.56 is found in Fig. 2(a), close to the theoretically predicted $e^{\alpha=0.5} \approx 1.65$ under consideration of the finite size effect, which is verified by the finite-size scaling analysis in Fig. 2(d). Figures 2(b) and 2(c) typically show the skin mode, which is exponentially decaying from one boundary, and the asymmetrically localized mode with different decaying lengths on both sides, respectively.

IV. PHASE TRANSITION AND WINDING NUMBERS UNDER PBCS

Because of the breakdown of the conventional bulk-boundary correspondence, the behaviors under PBCs and OBCs should be much different. However, the insensitivity of the localized states to the boundaries hints that the onset of AL under both boundary conditions should be identical. This judgment is numerically verified in Fig. 3(a): A steep rise of $\overline{\mathrm{IPR}}$ around e^{α}. Different from OBCs, the $\overline{\mathrm{IPR}}$ keeps low prior to the transition due to the lacking of the localized skin modes [Fig. 3(b)], while the localized states possess the same feature as OBCs [Fig. 3(c)].

Another big difference is the presence of imaginary eigenenergies [Fig. 3(d)]; the emergence of corner entries in h invalidates the similarity to a Hermitian matrix. This feature is intimately related to the phase transition if we are reminded that the localized states are insensitive to boundaries, preserving real eigenenergies: The complexity-reality transition of eigenenergies coincides with ALs. Using this tie, we may establish a *bulk-bulk* correspondence between systems under OBCs and PBCs through a winding number with respect to complex eigenenergies.

The conventional winding number cannot be used here because the chiral symmetry is broken by the on-site quasiperiodic potential [51,61]. Thus, we consider the ring chain with a magnetic flux $-\Phi$ penetrating through the center, yielding

$$\hat{H}(\Phi) = \hat{H} + J_R e^{-i\Phi}|1\rangle\langle N| + J_L e^{i\Phi}|N\rangle\langle 1|, \tag{6}$$

and the winding number is defined as [54]

$$\nu = \int_0^{2\pi} \frac{\partial_\Phi \ln\det \hat{H}(\Phi)}{2\pi i} \mathrm{d}\Phi = \int_0^{2\pi} \frac{\partial_\Phi \theta(\Phi)}{2\pi} \mathrm{d}\Phi, \tag{7}$$

where $\theta(\Phi)$ is the argument of $\det\hat{H}(\Phi)$. Apparently, $\nu = 0$ for the localized phase on account of the reality of the spectrum.

Figure 3(e) show numerically how $\theta(\Phi)$ changes with Φ from 0 to 2π in the three phases of Fig. 1(b), and the corresponding winding numbers are obtained. The phase boundaries can alternatively be determined by analyzing the asymptotic behavior of $\det H(\Phi)$ (see details in Appendix B). As a result, the chirality of the winding number can exactly tell the left/right-skin phases ($\nu = \pm 1$) and the localized phase ($\nu = 0$) under OBCs. Different from the conventional

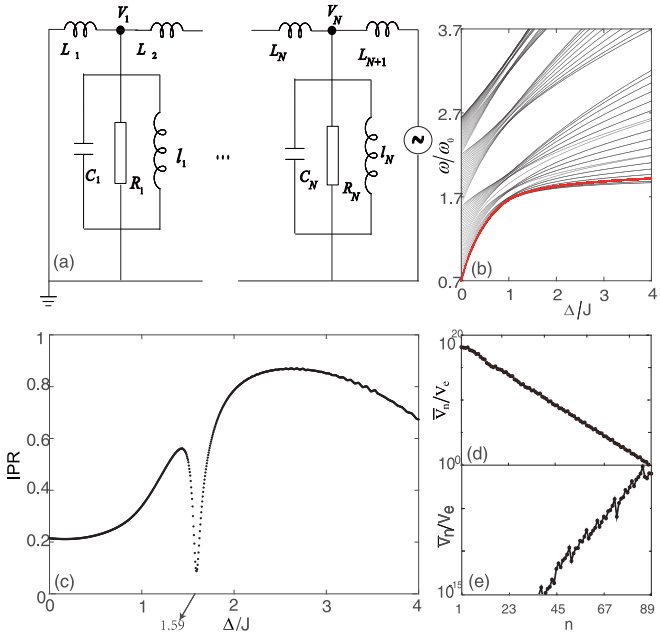

FIG. 4. (a) Schematic of the driven RLC electrical circuit with parameters defined in the text. (b) Intrinsic eigenfrequencies ω/ω_0 vs Δ/J for $\alpha = 0.5$. (c) IPR of $\overline{\mathcal{V}}$ vs Δ/J with driving frequencies indicated by the red curve in (b). The dive as in Fig. 2(a) indicates the transition point. (d),(e) Typical plots of $\overline{V}_n/V_e$ in (c) for $(\Delta/J, \tilde{\Omega}) = (0.5, 1.38)$ and (3,1.88), showing the amplifying and insulation in transport induced by NHSEs and ALs, respectively. $N = 89$ and $\beta = 55/89$ are used.

bulk-boundary correspondence, where edge states under OBCs can be predicted by a topological invariant defined under PBCs, here we establish a *bulk-bulk* correspondence, where the behavior of bulk states under OBCs can be predicted by a topological invariant defined under PBCs.

V. ELECTRICAL CIRCUIT'S REALIZATION

We propose a driven RLC electrical circuit for the nonreciprocal AA model under OBCs, as shown in Fig. 4(a), where inductors with inductances $L_n = Lg^{-n}$ and $l_n = Lg^{-n}[2\Delta(\cos 2\pi\beta n + 1)]^{-1}$, capacitors with capacitance $C_n = Cg^n$, and resistors with resistance $R_n = Rg^{-n}$ are all linear *passive* elements with positive free parameters, L, C, R, and g. The leftmost node is grounded for an open boundary while the other is connected to a voltage source of a continuous wave, $V_e(t) = V_e \sin(\Omega t)$, with driving frequency Ω.

Without resistors, the intrinsic eigenfrequency ω can be obtained by grounding the rightmost node instead of the source. Based on Kirchhoff's current law, the equation reads

$$V_{n-1} + gV_{n+1} - \Delta_n V_n = \left(f - \omega^2/\omega_0^2\right)V_n, \tag{8}$$

where V_n is the amplitude of the voltage $V_n(t)$ on node n, $f = 1 + g + 2\Delta$, and $\omega_0 = 1/\sqrt{LC}$. Rewritten in matrix form, $\mathcal{H}\mathcal{V} = E\mathcal{V}$, where $\mathcal{V} = (\{V_n\})^T$ is a column vector and $E = f - \omega^2/\omega_0^2$ is the eigenvalue. $\mathcal{H}$ is just the matrix representation of the nonreciprocal AA model (1) under OBCs with $J_L = g$ and $J_R = 1$. Notably, this classical circuit can only have real E, which is consistent with the previous proof. Figure 4(b) shows the intrinsic eigenfrequencies ω/ω_0 versus Δ/J with $J = \sqrt{g}$ and $\alpha = (\ln g)/2$.

When driving the system, the transport of continuous waves in different phases can be detected; the introduction of resistors in the following is for the system to quickly stabilize. The dynamical equation reads

$$\frac{d^2}{d\tau^2}\mathcal{V}(\tau) + \gamma\frac{d}{d\tau}\mathcal{V}(\tau) - (\mathcal{H} - f)\mathcal{V}(\tau) = \mathcal{V}_e \sin\tilde{\Omega}\tau, \tag{9}$$

where $\gamma = \frac{1}{R}\sqrt{\frac{L}{C}} > 0$ and $\tau = \omega_0 t$ are dimensionless, $\mathcal{V}_e = (0, ..., 0, V_e)^T$. '$\sim$' over frequencies hereafter means the frequency is dimensionless in unit of ω_0. The solution is

$$\mathcal{V}(\tau) = \sum_s \mathcal{V}_s\big[e^{-\gamma\tau/2}(c_s\cos\lambda_s\tau + d_s\sin\lambda_s\tau) + \mathcal{W}_s^T\mathcal{V}_e(a_s\cos\tilde{\Omega}\tau + b_s\sin\tilde{\Omega}\tau)\big], \tag{10}$$

where $a_s = \frac{\gamma\tilde{\Omega}}{\gamma^2\tilde{\Omega}^2 + (\tilde{\Omega}^2 - \tilde{\omega}_s^2)^2}$, $b_s = \frac{\tilde{\Omega}^2 - \tilde{\omega}_s^2}{\gamma^2\tilde{\Omega}^2 + (\tilde{\Omega}^2 - \tilde{\omega}_s^2)^2}$, $\lambda_s = \sqrt{\tilde{\omega}_s^2 - \gamma^2/2}$, and (c_s, d_s) are coefficients determined by initial conditions. $\mathcal{V}_s$ and $\mathcal{W}_s^T$ are sth right and left eigenvectors of $\mathcal{H}$, respectively, satisfying $\mathcal{W}_s^T\mathcal{V}_{s'} = \delta_{ss'}$. Note that if $\mathcal{V}_s$ is accumulated to one boundary, $\mathcal{W}_s$ is to the other because $\mathcal{W}_s$ is the right eigenvector of $\mathcal{H}^T$. Thus, to detect *left* skin modes, the source should be connected to the *right* end for the possible large overlap $\mathcal{W}_s^T\mathcal{V}_e$. It is much different from Hermitian cases, where the source must be on the same side. In Eq. (10), the first part in the square brackets is the general solution, which, due to resistors, will decay in a long time limit and thus, the effect of initial conditions can be ignored; the second part is one specific solution, which is stable, oscillating with the driving frequency. Moreover, if $\gamma \ll 1$, the system is resonant when $\Omega \approx \omega_s$ with a large value of a_s and vanishing b_s, unless the overlap $\mathcal{W}_s^T\mathcal{V}_e$ is zero, and the corresponding right eigenvector $\mathcal{V}_s$ can be picked out.

The IPR of the time-averaged voltage vector, $\overline{\mathcal{V}} = \frac{1}{T}\int_\tau^{\tau+T}|\mathcal{V}(\tau)|\mathrm{d}\tau$ with $T = 2\pi/\tilde{\Omega}$ in $\tau \to \infty$ limit, is shown in Fig. 4(c), where a deep dive at $\sim$1.59 is close to the transition point. Figures 4(d) and 4(e) plot the typical transports in both phases at $\alpha = 0.5$: In the skin phase, due to the existence of left-skin modes, the continuous wave is resonantly transferred and accumulated to the left boundary; while in the localized phase, because of the small overlap $\mathcal{W}_s^T\mathcal{V}_e$, the wave is confined to the right boundary without resonance. If the input is on the left, also because of the small overlap $\mathcal{W}_s^T\mathcal{V}_e$, the signal cannot resonate and still localize on the left. This indicates that NHSEs can enhance the wave transport and may be useful in applications. This paradigmatic scheme of nonreciprocity can be immediately applied to other nonreciprocal models, e.g., the nonreciprocal Su-Schrieffer-Heeger model [49–52].

VI. DISCUSSION AND CONCLUSION

The phase diagram in Fig. 1(b) is obtained for positive hoppings. For general complex hoppings with arbitrary phases $\phi_{R(L)}$, an identical phase diagram is found numerically. Although there is no proper way to relate it to the positive-hopping case due to the effective net flux between each two

nearest-neighbor sites, the special case satisfying $\phi_R + \phi_L = n\pi$ ($n \in$ integer) can be proved exactly by the duality. We note that this transformation can map the nonreciprocal model to the AA model with complex on-site potentials, which, in a new basis, shares a similar AL but has no NHSEs. See details in Appendix A.

For the circuit's realization, the element values can be typically taken as $L \sim$ mH, $C \sim$ pF, and $R \sim$ kΩ, i.e., $\omega_0 = 1/\sqrt{LC} \sim$ kHz, which is accessible in usual experiments [75–83]. For typical nonreciprocal hoppings, say $\alpha = 0.2$ and thus $g = e^{0.4} \approx 1.49$, the element values can still drop in almost the same orders for $N = 10$ sites with $L_n \sim \mu$H to mH, $C_n \sim$ pF, and $R_n \sim$ kΩ.

In summary, we have studied the topological transition of NHSEs and ALs in nonreciprocal AA models and obtained the exact phase diagram. Moreover, an electrical circuit has been proposed to demonstrate the transition properties. This paradigmatic scheme can be straightforwardly applied to more nonreciprocal models and may be generalized to other artificial platforms, opening the window of studying the interplay of NHSEs and ALs as well as other exotic quantum/topological phenomena.

ACKNOWLEDGMENTS

S.C. was supported by the NSFC (Grant No. 11425419) and the NKRDP of China (Grant No. 2016YFA0300600 and No. 2016YFA0302104). L.-J.L. was supported by the startup funding from SCNU. S.-L.Z. was supported by the NSFC (Grant Nos. 91636218 and U1801661), the NKRDP of China (Grant No. 2016YFA0301803), and the Key Program of Science and Technology of Guangzhou (Grant No. 201804020055).

APPENDIX A: DUALITY

That the nonreciprocal AA model can be transformed to an AA model with a complex on-site potential, i.e., the duality, can work in two cases: (1) Under PBCs with $\beta = p/N$, where $p \in$ integer; (2) under OBCs with $N \to \infty$, because these two cases can ensure that the transformed k space is closed by the following Fourier transform.

First, let's deal with Hamiltonian (6) in the main text. By a gauge transformation $|n\rangle \to e^{-i\Phi n/N}|n\rangle$, Hamiltonian (6) becomes

$$H(\Phi) = \sum_n [J_R e^{-i\Phi/N}|n+1\rangle\langle n| + J_L e^{i\Phi/N}|n\rangle\langle n+1| + \Delta_n|n\rangle\langle n|]. \tag{A1}$$

Then, a Fourier transform, $|n\rangle = \frac{1}{\sqrt{N}}\sum_k e^{-i2\pi\beta kn}|k\rangle$, can further change it to the k space,

$$H(\Phi) = \sum_k [\Delta(|k+1\rangle\langle k| + |k\rangle\langle k+1|) + J_k(\Phi)|k\rangle\langle k|], \tag{A2}$$

where $J_k(\Phi) = 2J[\cosh\alpha\cos(2\pi\beta k + \Phi/N) - i\sinh\alpha\sin(2\pi\beta k + \Phi/N)]$. Note that the quasimomentum is $2\pi\beta k$, not the index k; the hopping terms actually couple the two quasimomenta with difference $2\pi\beta$. Due to the PBCs, the quasimomentum should satisfy $2\pi\beta k = 2\pi m/N$, i.e., $k = m/\beta N$, where $m \in$ integer. To make the Hilbert space closed, we can just set $\beta = p/N$, and thus, $k + 1 = (m + p)/p$ corresponds to another quasimomentum index in the same Hilbert space, if considering the periodicity of the Brillouin zone. In this sense, the two dual models, Eqs. (A1) and (A2), are equivalent with identical energy spectra.

Secondly, consider the Hamiltonian (1) in the main text under OBCs with infinite length, i.e., $N \to \infty$. The dual Hamiltonian in k space has the same form as Eq. (A2) with only the difference that $\Phi = 0$ and the boundaries are open. When $J_R = J_L = J$, i.e., $\alpha = 0$, the dual Hamiltonians have the same form and thus $\det h'(\Delta, J) = \det h'(J, \Delta)$, i.e., $J^N \det h'(\Delta/J) = \Delta^N \det h'(J/\Delta)$. Note that $\det h = \det h'$ because of their similarity, we have the relation that $\det h(\Delta/J) = (\Delta/J)^N \det h(J/\Delta)$. We have noted that Ref. [69] *numerically* gives the condition for the AL of the on-site complex AA model (A2), $|J/\Delta \cdot \cosh\alpha| + |J/\Delta \cdot \sinh\alpha| = 1$, i.e., $\Delta/J = e^{|\alpha|}$, which is consistent with our result in the main text.

APPENDIX B: CALCULATION OF THE WINDING NUMBER

We calculate the winding number (7) of Hamiltonian (6) in the main text. In matrix form, it can be rewritten as

$$\hat{H}_\Phi = \sum_{mn} h_{mn}(\Phi)|m\rangle\langle n|, \tag{B1}$$

where $h_{mn}(\Phi)$ is the entry of the following matrix,

$$h(\Phi) = \begin{pmatrix} \Delta_1 & J_L & & & J_R e^{-i\Phi} \\ J_R & \Delta_2 & J_L & & \\ & \ddots & \ddots & \ddots & \\ & & J_R & \Delta_{N-1} & J_L \\ J_L e^{i\Phi} & & & J_R & \Delta_N \end{pmatrix}. \tag{B2}$$

The key to calculate the winding number is the determinant of $h(\Phi)$. Mathematically, we have

$$\begin{aligned} \det h(\Phi) &= -(-J_L)^N e^{i\Phi} - (-J_R)^N e^{-i\Phi} + P \\ &= -2(-J)^N(\cosh\alpha N\cos\Phi \\ &\quad + i\sinh\alpha N\sin\Phi) + P, \end{aligned} \tag{B3}$$

where $P = \det h' - J^2 \det u'$ with h' being defined in Eq. (2) in the main text and u' is a submatrix with $(N-2)$ dimension of h' by removing the first and last row and column. Apparently, P is real.

Because the winding number (7) defined in the main text reveals how $\det\hat{H}(\Phi)$ evolves with respect to Φ from 0 to 2π in the complex plane, we can rewrite the winding number with the aid of the sign operators [61],

$$\nu = \frac{1}{2}\sum_i \mathrm{sgn}[x(\Phi_i)]\cdot\mathrm{sgn}\left[\frac{dy(\Phi_i)}{d\Phi}\right], \tag{B4}$$

where $x = \mathrm{Re}[\det h(\Phi)] = P - 2(-J)^N\cosh\alpha N\cos\Phi$ and $y = \mathrm{Im}[\det h(\Phi)] = -2(-J)^N\sinh\alpha N\sin\Phi$. Φ_i is the ith solution of $y(\Phi) = 0$, which are $\Phi_1 = 0$ and $\Phi_2 = \pi$. Therefore,

we have

$$\begin{aligned}\nu &= \frac{(-1)^N \mathrm{sgn}(\alpha)}{2}[\mathrm{sgn}(P+2(-J)^N\cosh\alpha N)\\ &\quad -\mathrm{sgn}(P-2(-J)^N\cosh\alpha N)]\\ &= \mathrm{sgn}(\alpha)\theta(2J^N\cosh\alpha N-|P|).\end{aligned} \tag{B5}$$

The transition point is determined by

$$|P| = 2J^N\cosh\alpha N \approx J^N e^{|\alpha|N}, \tag{B6}$$

i.e.,

$$\mathcal{P} \equiv \sqrt[N]{|P|} \approx Je^{|\alpha|}, \tag{B7}$$

where the squiggly equal sign is for the large N limit. To calculate P, we can expand it [20] as

$$P = \sum_{n=0}^{[N/2]} c_{N-2n}(-1)^n J^{2n}(2\Delta)^{N-2n}, \tag{B8}$$

where $[N/2]$ means the nearest integer less than $N/2$, and

$$c_{N-2n} = \sum_{\substack{\{j_s,\, j_s+1\}\\ (s=1,\cdots,n)}} \prod_{\substack{i=1\\ i\neq j_s,\, j_s+1,\\ (s=1,\cdots,n)}}^{N} \cos(2\pi\beta i), \tag{B9}$$

where the first summation is over all possible configurations $\{j_1, j_1+1, \cdots, j_n, j_n+1\}$ with nonrepetitive index $j_s \in [1, N)$. For the coefficient $c_N = \prod_{i=1}^{N}\cos(2\pi\beta i)$, we have

$$\begin{aligned}\lim_{N\to\infty}\ln c_N &= \lim_{N\to\infty}\sum_{i=1}^{N}\ln\cos(2\pi\beta i)\\ &= N\int_0^1 \ln\cos(2\pi\beta N x)dx\\ &= -\frac{1}{2\pi\beta}\mathcal{L}(2\pi\beta N) \approx -N\ln 2\end{aligned} \tag{B10}$$

where $\mathcal{L}(x)$ is the Lobachevskiy's function defined as [86]

$$\begin{aligned}\mathcal{L}(x) &= -\int_0^x \ln\cos(x')dx'\\ &= x\ln 2 - \frac{1}{2}\sum_{k=1}^{\infty}(-1)^{k-1}\frac{\sin(2kx)}{k^2}.\end{aligned} \tag{B11}$$

This means in the limit $N\to\infty$, $c_N \sim 2^{-N}$. In the same way, $c_{N-2} \sim 2^{-(N-2)}$. Thus, using Eq. (B8), we have

$$\mathcal{P} = J\left[\left|c_N\left(\frac{2\Delta}{J}\right)^N - c_{N-2}\left(\frac{2\Delta}{J}\right)^{N-2} + \ldots\right|\right]^{\frac{1}{N}}. \tag{B12}$$

For $\Delta/J \leqslant 1$, $\lim_{N\to\infty}\mathcal{P} = J$, and thus $\nu = \mathrm{sgn}(\alpha)$, while for $\Delta/J > 1$, $\lim_{N\to\infty}\mathcal{P} = \Delta$ and thus $\nu = \mathrm{sgn}(\alpha)\theta(Je^{|\alpha|} - \Delta)$, that is, when $e^{|\alpha|} < \Delta/J$, $\nu = 0$ and when $e^{|\alpha|} > \Delta/J$, $\nu = \mathrm{sgn}(\alpha)$. The boundary of the topologically trivial and nontrivial phases is determined by $\Delta/J = e^{|\alpha|}$, which is consistent with the result from the point of view of the localization-delocalization transition in the main text.

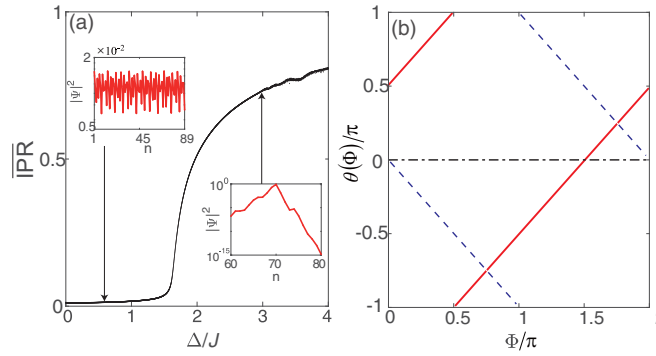

FIG. 5. Phase transition for $(\phi_R, \phi_L) = (0, \pi/2)$. (a) $\overline{\mathrm{IPR}}$ vs Δ/J for $\alpha = 0.5$ under PBCs. Insets: The profiles of the eigenstates of 10th lowest $|E|$, showing the NHSE and the AL at $\Delta/J = 0.5$ and 3, respectively. (b) $\theta(\Phi)$ for $\alpha = \Delta/J = 0.5$ (solid red), $\alpha = -\Delta/J = -0.5$ (dashed blue), and $\alpha = 0$, $\Delta/J = 3$ (dash-dotted black), which correspond to $\nu = +1$, -1, and 0, respectively. The calculation is carried on with $N = 89$ and $\beta = 55/89$.

APPENDIX C: GENERAL CASE WITH COMPLEX HOPPINGS

We paid attention to the typical case of positive J_L and J_R in Hamiltonian (1) of the main text. Here we show that the general case is related to this special case, and thus share the same transition point on AL.

The Hamiltonian with arbitrary complex hoppings reads

$$\begin{aligned}\hat{H}_{\mathrm{gel}} = \sum_n (&J_R e^{i\phi_R}|n+1\rangle\langle n| + J_L e^{i\phi_L}|n\rangle\langle n+1|\\ &+\Delta_n|n\rangle\langle n|),\end{aligned} \tag{C1}$$

where $J_{R(L)} > 0$ and Δ_n keep the same definitions as in Hamiltonian (1) of the main text, and $\phi_{R(L)}$ is the arbitrary argument of the corresponding hopping. To reveal the relation between the general case of hoppings and the positive case, we do the following gauge transformation, which does not change the energy spectrum,

$$\begin{aligned}\hat{U}\hat{H}_{\mathrm{gel}}\hat{U}^{-1} = e^{i\frac{\phi_R+\phi_L}{2}}\sum_n \big(&\Delta_n e^{-i\frac{\phi_R+\phi_L}{2}}|n\rangle\langle n|\\ &+J_R|n+1\rangle\langle n| + J_L|n\rangle\langle n+1|\big),\end{aligned} \tag{C2}$$

where $\hat{U}$ is a unitary operator defined by $\hat{U}|n\rangle = e^{i\frac{\phi_L-\phi_R}{2}n}|n\rangle$. Except for the overall phase and the phase of on-site terms, the above transformed Hamiltonian is similar to Hamiltonian (1) of the main text.

Specifically, when $\phi_R + \phi_L = 2n\pi$ (n $\in$ integer), we have

$$\hat{H}_{\mathrm{gel}} = (-1)^n\hat{U}^{-1}\hat{H}\hat{U} \tag{C3}$$

where $\hat{H}$ is just the Hamiltonian (1) in the main text. Apparently, the phase boundaries of this case is identical to the real-hopping case with only the eigenenergy E becoming $(-1)^n E$. Note that for odd n, the minus sign of on-site terms in Eq. (C2) can be absorbed to the cosine terms in Δ_n by shifting a phase, which makes no difference for the infinite chain.

For the general case, we cannot find a relation to the positive real-hopping case, which can be understood by noting

that the right and left hoppings generally generate a net flux, $\phi_L + \phi_R$, for each two nearest-neighbor sites, as there seems a coil in between with a magnetic field through it, and thus, the phase cannot be gauged away. However, the phase diagrams seem the same by our numerical calculation, which can also be characterized by the winding number, as shown in Fig. 5.

[1] P. W. Anderson, Phys. Rev. **109**, 1492 (1958).
[2] Edited by E. Abrahams, *50 Years of Anderson Localization*, 1st ed. (World Scientific, Singapore, 2010).
[3] P. A. Lee and T. V. Ramakrishnan, Rev. Mod. Phys. **57**, 287 (1985).
[4] G. Feher, Phys. Rev. **114**, 1219 (1959).
[5] G. Feher and E. A. Gere, Phys. Rev. **114**, 1245 (1959).
[6] D. S. Wiersma, P. Bartolini, A. Lagendijk, and R. Righini, Nature (London) **390**, 671 (1997).
[7] F. Scheffold, R. Lenke, R. Tweer, and G. Maret, Nature (London) **398**, 206 (1999).
[8] T. Schwartz, G. Bartal, S. Fishman, and M. Segev, Nature (London) **446**, 52 (2007).
[9] C. M. Aegerter, M. Störzer, S. Fiebig, W. Bührer, and G. Maret, J. Opt. Soc. Am. A **24**, A23 (2007).
[10] R. Dalichaouch, J. P. Armstrong, S. Schultz, P. M. Platzman, and S. L. McCall, Nature (London) **354**, 53 (1991).
[11] A. A. Chabanov, M. Stoytchev, and A. Z. Genack, Nature (London) **404**, 850 (2000).
[12] P. Pradhan and S. Sridhar, Phys. Rev. Lett. **85**, 2360 (2000).
[13] R. L. Weaver, Wave Motion **12**, 129 (1990).
[14] J. Billy, V. Josse, Z. Zuo, A. Bernard, B. Hambrecht, P. Lugan, D. Clement, L. Sanchez-Palencia, P. Bouyer, and A. Aspect, Nature (London) **453**, 891 (2008).
[15] G. Roati, C. D'Errico, L. Fallani, M. Fattori, C. Fort, M. Zaccanti, G. Modugno, M. Modugno, and M. Inguscio, Nature (London) **453**, 895 (2008).
[16] H. P. Lüschen, S. Scherg, T. Kohlert, M. Schreiber, P. Bordia, X. Li, S. Das Sarma, and I. Bloch, Phys. Rev. Lett. **120**, 160404 (2018).
[17] S. Aubry and G. André, Ann. Israel Phys. Soc. **3**, 133 (1980).
[18] L.-J. Lang, X. Cai, and S. Chen, Phys. Rev. Lett. **108**, 220401 (2012).
[19] F. Mei, S.-L. Zhu, Z.-M. Zhang, C. H. Oh, and N. Goldman, Phys. Rev. A **85**, 013638 (2012).
[20] X. Cai, L.-J. Lang, S. Chen, and Y. Wang, Phys. Rev. Lett. **110**, 176403 (2013).
[21] Z. Xu, L. Li, and S. Chen, Phys. Rev. Lett. **110**, 215301 (2013).
[22] S.-L. Zhu, Z.-D. Wang, Y.-H. Chan, and L.-M. Duan, Phys. Rev. Lett. **110**, 075303 (2013).
[23] D. R. Hofstadter, Phys. Rev. B **14**, 2239 (1976).
[24] D. J. Thouless, Phys. Rev. B **27**, 6083 (1983).
[25] Y. E. Kraus, Y. Lahini, Z. Ringel, M. Verbin, and O. Zilberberg, Phys. Rev. Lett. **109**, 106402 (2012).
[26] M. Lohse, C. Schweizer, O. Zilberberg, M. Aidelsburger, and I. Bloch, Nat. Phys. **12**, 350 (2016).
[27] S. Nakajima, T. Tomita, S. Taie, T. Ichinose, H. Ozawa, L. Wang, M. Troyer, and Y. Takahashi, Nat. Phys. **12**, 296 (2016).
[28] N. Moiseyev, *Non-Hermitian Quantum Mechanics*, 1st ed. (Cambridge University Press, Cambridge, 2011).
[29] L. Lu, J. D. Joannopoulos, and M. Soljacic, Nat. Photonics **8**, 821 (2014).
[30] T. Ozawa, H. M. Price, A. Amo, N. Goldman, M. Hafezi, L. Lu, M. C. Rechtsman, D. Schuster, J. Simon, O. Zilberberg, and I. Carusotto, Rev. Mod. Phys. **91**, 015006 (2019).
[31] Y. Wang, Y.-H. Lu, F. Mei, J. Gao, Z.-M. Li, H. Tang, S.-L. Zhu, S. Jia, and X.-M. Jin, Phys. Rev. Lett. **122**, 193903 (2019).
[32] C. M. Bender and S. Boettcher, Phys. Rev. Lett. **80**, 5243 (1998).
[33] A. Guo, G. J. Salamo, D. Duchesne, R. Morandotti, M. Volatier-Ravat, V. Aimez, G. A. Siviloglou, and D. N. Christodoulides, Phys. Rev. Lett. **103**, 093902 (2009).
[34] B. Peng, S. K. Ozdemir, F. Lei, F. Monifi, M. Gianfreda, G. L. Long, S. Fan, F. Nori, C. M. Bender, and L. Yang, Nat. Phys. **10**, 394 (2014).
[35] B. Zhen, C. W. Hsu, Y. Igarashi, L. Lu, I. Kaminer, A. Pick, S.-L. Chua, J. D. Joannopoulos, and M. Soljacic, Nature (London) **525**, 354 (2015).
[36] K. Ding, G. Ma, M. Xiao, Z. Q. Zhang, and C. T. Chan, Phys. Rev. X **6**, 021007 (2016).
[37] J. Doppler, A. A. Mailybaev, J. Bohm, U. Kuhl, A. Girschik, F. Libisch, T. J. Milburn, P. Rabl, N. Moiseyev, and S. Rotter, Nature (London) **537**, 76 (2016).
[38] H. Xu, D. Mason, L. Jiang, and J. G. E. Harris, Nature (London) **537**, 80 (2016).
[39] B. Midya, H. Zhao, and L. Feng, Nat. Commun. **9**, 2674 (2018).
[40] M. S. Rudner and L. S. Levitov, Phys. Rev. Lett. **102**, 065703 (2009).
[41] Y. C. Hu and T. L. Hughes, Phys. Rev. B **84**, 153101 (2011).
[42] K. Esaki, M. Sato, K. Hasebe, and M. Kohmoto, Phys. Rev. B **84**, 205128 (2011).
[43] B. Zhu, R. Lü, and S. Chen, Phys. Rev. A **89**, 062102 (2014).
[44] T. E. Lee, Phys. Rev. Lett. **116**, 133903 (2016).
[45] D. Leykam, K. Y. Bliokh, C. Huang, Y. D. Chong, and F. Nori, Phys. Rev. Lett. **118**, 040401 (2017).
[46] L. Jin, Phys. Rev. A **96**, 032103 (2017).
[47] H. Shen, B. Zhen, and L. Fu, Phys. Rev. Lett. **120**, 146402 (2018).
[48] S. Lieu, Phys. Rev. B **97**, 045106 (2018).
[49] C. Yin, H. Jiang, L. Li, R. Lü, and S. Chen, Phys. Rev. A **97**, 052115 (2018).
[50] S. Yao and Z. Wang, Phys. Rev. Lett. **121**, 086803 (2018).
[51] Y. Xiong, J. Phys. Commun. **2**, 035043 (2018).
[52] F. K. Kunst, E. Edvardsson, J. C. Budich, and E. J. Bergholtz, Phys. Rev. Lett. **121**, 026808 (2018).
[53] V. M. Martinez Alvarez, J. E. Barrios Vargas, and L. E. F. Foa Torres, Phys. Rev. B **97**, 121401(R) (2018).
[54] Z. Gong, Y. Ashida, K. Kawabata, K. Takasan, S. Higashikawa, and M. Ueda, Phys. Rev. X **8**, 031079 (2018).
[55] S. Yao, F. Song, and Z. Wang, Phys. Rev. Lett. **121**, 136802 (2018).
[56] L. Jin and Z. Song, Phys. Rev. B **99**, 081103 (2019).
[57] C. H. Lee and R. Thomale, Phys. Rev. B **99**, 201103 (2019).
[58] K. Kawabata, K. Shiozaki, and M. Ueda, Phys. Rev. B **98**, 165148 (2018).

[59] C. H. Lee, L. Li, and J. Gong, Phys. Rev. Lett. **123**, 016805 (2019).
[60] L.-J. Lang, Y. Wang, H. Wang, and Y. D. Chong, Phys. Rev. B **98**, 094307 (2018).
[61] H. Jiang, C. Yang, and S. Chen, Phys. Rev. A **98**, 052116 (2018).
[62] G. Harari, M. A. Bandres, Y. Lumer, M. C. Rechtsman, Y. D. Chong, M. Khajavikhan, D. N. Christodoulides, and M. Segev, Science **359**, eaar4003 (2018).
[63] M. A. Bandres, S. Wittek, G. Harari, M. Parto, J. Ren, M. Segev, D. N. Christodoulides, and M. Khajavikhan, Science **359**, eaar4005 (2018).
[64] N. Hatano and D. R. Nelson, Phys. Rev. Lett. **77**, 570 (1996).
[65] N. Hatano and D. R. Nelson, Phys. Rev. B **56**, 8651 (1997).
[66] N. M. Shnerb and D. R. Nelson, Phys. Rev. Lett. **80**, 5172 (1998).
[67] N. Moiseyev and M. Glück, Phys. Rev. E **63**, 041103 (2001).
[68] J. Heinrichs, Phys. Rev. B **63**, 165108 (2001).
[69] A. Jazaeri and I. I. Satija, Phys. Rev. E **63**, 036222 (2001).
[70] S. Longhi, J. Phys. A **47**, 165302 (2014).
[71] C. Yuce, Phys. Lett. A **378**, 2024 (2014).
[72] C. H. Liang, D. D. Scott, and Y. N. Joglekar, Phys. Rev. A **89**, 030102(R) (2014).
[73] Q.-B. Zeng, S. Chen, and R. Lü, Phys. Rev. A **95**, 062118 (2017).
[74] Q.-B. Zeng, Y.-B. Yang, and Y. Xu, arXiv:1901.08060.
[75] J. Ningyuan, C. Owens, A. Sommer, D. Schuster, and J. Simon, Phys. Rev. X **5**, 021031 (2015).
[76] C. H. Lee, S. Imhof, C. Berger, F. Bayer, J. Brehm, L. W. Molenkamp, T. Kiessling, and R. Thomale, Commun. Phys. **1**, 39 (2018).
[77] S. Imhof, C. Berger, F. Bayer, J. Brehm, L. W. Molenkamp, T. Kiessling, F. Schindler, C. H. Lee, M. Greiter, T. Neupert, and R. Thomale, Nat. Phys. **14**, 925 (2018).
[78] Y. Hadad, J. C. Soric, A. B. Khanikaev, and A. Alu, Nature Electronics **1**, 178 (2018).
[79] Y. Li, Y. Sun, W. Zhu, Z. Guo, J. Jiang, T. Kariyado, H. Chen, and X. Hu, Nat. Commun. **9**, 4598 (2018).
[80] K. Luo, R. Yu, and H. Weng, Research **2018**, 10 (2018).
[81] Y. Wang, L.-J. Lang, C. H. Lee, B. Zhang, and Y. D. Chong, Nat. Commun. **10**, 1102 (2019).
[82] Y. Lu, N. Jia, L. Su, C. Owens, G. Juzeliūnas, D. I. Schuster, and J. Simon, Phys. Rev. B **99**, 020302(R) (2019).
[83] M. Serra-Garcia, R. Süsstrunk, and S. D. Huber, Phys. Rev. B **99**, 020304(R) (2019).
[84] D.-W. Zhang, Y.-Q. Zhu, Y. X. Zhao, H. Yan, and S.-L. Zhu, Adv. Phys. **67**, 253 (2018).
[85] X. Gu, A. F. Kockum, A. Miranowicz, Y.-x. Liu, and F. Nori, Phys. Rep. **718-719**, 1 (2017).
[86] I. S. Gradshteyn and I. M. Ryzhik, *Table of Integrals, Series, and Products*, 7th ed., edited by A. Jeffrey and D. Zwillinger (Academic Press/Elsevier, Oxford, 2007).